THE JOURNAL OF BIOLOGICAL CHEMISTRY Vol. 270, No. 42, Issue of October 20, pp. 25047–25056, 1995
Printed in U.S.A.

Molecular Cloning, Expression, Chromosomal Assignment, and Tissue-specific Expression of a Murine α-(1,3)-Fucosyltransferase Locus Corresponding to the Human ELAM-1 Ligand Fucosyl Transferase*

(Received for publication, July 14, 1995)

Kevin M. Gersten‡§¶, Shunji Natsuka‡, Marco Trinchera‖, Bronislawa Petryniak‡, Robert J. Kelly‡, Nozomu Hiraiwa‡, Nancy A. Jenkins, Debra J. Gilbert**, Neal G. Copeland**, and John B. Lowe‡‖‡‡**

*From the ‡Howard Hughes Medical Institute, the ‖Department of Pathology, and the ¶Cell and Molecular Biology Program, the University of Michigan Medical School, Ann Arbor, Michigan 48109-0650 and the **Mammalian Genetics Laboratory, Advanced Biosciences Laboratory, Inc. Basic Research Program, National Cancer Institute, Frederick Cancer Research and Development Center, Frederick, Maryland 21702*

Terminal Fucα1–3GlcNAc moieties are displayed by mammalian cell surface glycoconjugates in a tissue-specific manner. These oligosaccharides participate in selectin-dependent leukocyte adhesion and have been implicated in adhesive events during murine embryogenesis. Other functions for these molecules remain to be defined, as do the tissue-specific expression patterns of the corresponding α-(1–3)-fucosyltransferase (α1–3FT) genes. This report characterizes a murine α1–3FT that shares 77% amino acid sequence identity with human ELAM ligand fucosyltransferase (ELFT, also termed Fuc-TIV). The corresponding gene maps to mouse chromosome 9 in a region of homology with the Fuc-TIV locus on human chromosome 11q. *In vitro*, the murine α1–3FT can efficiently fucosylate the trisaccharide Galα1–3Galβ1–4GlcNAc (apparent K_m of 0.71 mM) to form an unusual tetrasaccharide (Galα1–3Galβ1–4[Fucα1–3]GlcNAc) described in periimplantation mouse tissues. The enzyme can also form the Lewis x determinant from Galβ1–4GlcNAc (K_m = 2.05 mM), and the sialyl Lewis x determinant from NeuNAcα2–3Galβ1–4GlcNAc (K_m = 1.78 mM). However, it does not yield sialyl Lewis x determinants when expressed in a mammalian cell line that maintains sialyl Lewis x precursors. Transcripts from this gene accumulate to low levels in hematopoietic organs, but are unexpectedly abundant in epithelia that line the stomach, small intestine, colon, and epididymus. Epithelial cell-specific expression of this gene suggests function(s) in addition to, and distinct from, its proposed role in selectin ligand synthesis.

Oligosaccharides represent major components of animal cell surfaces and are believed to function in cellular interactions during development and differentiation (1, 2), oncogenic transformation (3), and inflammation (4). Identification of specific oligosaccharide ligands for the selectin family of cell adhesion molecules directly links cell surface carbohydrates to cell-cell communication in the context of inflammatory response (5–7). The proposed ligands for E-selectin and P-selectin are fucosylated oligosaccharides (for review, see Refs. 4 and 8), whose biosynthesis is catalyzed by α-(1–3)-fucosyltransferases (α1–3FTs).[1] These enzymes are encoded by one or more distinct and tightly regulated α1–3FT genes.

Much of the interest in discovering functional roles for oligosaccharides during development is derived from studies documenting precise temporal-spatial expression patterns for some oligosaccharides during human and murine embryogenesis (9–12). The murine stage-specific embryonic antigen-1 (SSEA-1; (Galβ1–4[Fucα1–3]GlcNAc; Lewis x)), for example, is expressed coincident with morula compaction at the 8–16 cell stage of the preimplantation mouse embryo (13, 14). Since SSEA-1 structural analogs appear to inhibit compaction, it has been suggested that this antigen may participate in this process (1, 2). While it has been proposed that the SSEA-1 determinant functions to promote homotypic adhesion (15), neither the physiological relevance of this interaction during compaction nor the existence of other preimplantation-specific receptors for SSEA-1 have been demonstrated. Furthermore, it has not been possible to identify and directly demonstrate functional correlates for SSEA-1 expression patterns during early embryogenesis.

Virtually nothing is known about the molecular mechanisms that determine the tissue-specific and developmentally regulated expression patterns of the oligosaccharides implicated in morphogenic events during early murine embryogenesis. Expression of surface-localized SSEA-1 molecules may be regulated by differential expression of α1–3FT(s) required for their synthesis (16) and of sialyltransferases (17) and an α-(1–3)-

* This work was supported in part by National Institutes of Health Grant 1R01GM47455 (to J. B. L.) and by the National Cancer Institute, under contract NO1-CO-74101 with ABL (to N. A. J., and N. E. C). Computer-based DNA sequence analysis was supported in part by National Institutes of Health Grant M01RR00042 to the General Clinical Research Center at the University of Michigan. The costs of publication of this article were defrayed in part by the payment of page charges. This article must therefore be hereby marked "*advertisement*" in accordance with 18 U.S.C. Section 1734 solely to indicate this fact.

The nucleotide sequence(s) reported in this paper has been submitted to the GenBank™/EMBL Data Bank with accession number(s) U33457 and U33458.

§ Partially supported by the National Institutes of Health Predoctoral Training Grant 5T32GM07315 to the Cell and Molecular Biology Graduate Program at the University of Michigan.

‡‡ An Associate Investigator of the Howard Hughes Medical Institute. To whom correspondence should be addressed: Howard Hughes Medical Inst., Medical Science Research Bldg. I, Rm. 3510, 1150 W. Medical Center Dr., Ann Arbor, MI 48109-0650. Tel.: 313-747-4779; Fax: 313-936-1400.

[1] The abbreviations used are: α1–3FT, α-(1–3)-fucosyltransferase, ELFT, ELAM-1 ligand fucosyl transferase; FCS, fetal calf serum; MEL, murine erythroleukemia cell line; HPLC, high performance liquid chromatography; bp, base pair(s); kb, kilobase(s); GDP-fucose, β-D-*N*-acetylglucosaminide 3-α-L-fucosyltransferase.

galactosyltransferase (18) that may mask SSEA-1 expression (9, 10, 18). The relative contributions of these and other regulatory mechanisms, in the context of the developing embryo, remain undefined.

To begin to define, in detail, the enzymes and mechanisms that determine expression of Fucα1–3GlcNAc linkages in murine cell surface oligosaccharides, we have isolated and characterized a murine gene that corresponds to a human α1–3FT gene termed Fuc-TIV (Refs. 19 and 20; also known as ELFT for ELAM-1 ligand fucosyl transferase, Ref. 21). The mouse enzyme differs from human Fuc-TIV/ELFT in its relatively higher apparent affinity for α-(2–3)-sialylated type acceptor substrates *in vitro*, and is able to efficiently synthesize an unusual tetrasaccharide (Galα1–3Galβ1–4[Fucα1–3]GlcNAc) whose existence in periimplantation mouse tissues has been previously inferred (10). Northern blot analyses confirm that transcripts corresponding to this gene accumulate in leukocytic cell lines and in leukocyte-rich tissues in the mouse. However, these analyses, and companion *in situ* hybridization studies, demonstrate that Fuc-TIV/ELFT transcripts are unexpectedly abundant in epithelial cells lining the gastrointestinal and reproductive tracts and suggest that this sequence, and the cognate Fucα1–3GlcNAc linkages whose expression it determines may have unexpected functions in these tissues.

EXPERIMENTAL PROCEDURES

Cell Culture—COS-7 cells were grown in Dulbecco's modified Eagle's medium, 10% fetal calf serum (FCS). The murine B cell line S107 (22) and the murine T cell line EL4 (ATCC TIB 39, Ref. 23) were obtained from Dr. Jeffrey Leiden (University of Chicago). S107 cells were cultured in RPMI 1640 media, 10% FCS and 50 μM 2-mercaptoethanol. The EL4 line was maintained in RPMI 1640 media, 10% FCS. The B cell hybridoma lines TH2.54.63 (24) and 180.1 (25) were obtained from Dr. Wesley Dunnick (University of Michigan). The murine 180.1 cells were grown in RPMI 1640, 10% FCS while the TH2.54.63 cells were cultured in RPMI 1640, 5% FCS, 10% NCTC 109 (Gibco). The friend murine erythroleukemia cell line (MEL, Refs. 26 and 27) was provided by Dr. Michael Clark (University of Michigan) and cultured in Dulbecco's modified Eagle's medium, 10% FCS. The murine macrophage cell lines RAW264.7 (28, 29) and P388D_1 (ATCC TIB 63, Ref. 30) were provided by Dr. Steven Kunkel (University of Michigan). RAW264.7 cells were grown in Dulbecco's modified Eagle's medium, 10% FCS, while the P388D_1 cell line was maintained in RPMI 1640 media, 10% FCS.

Antibodies—Anti-Lewis x (anti-SSEA-1, mouse monoclonal IgM, ascites; Ref. 13) was provided by Davor Solter (Wistar Institute, Philadelphia, PA). Anti-H and anti-Lewis a antibodies (mouse IgM monoclonal, antigen-affinity purified) were purchased from Chembiomed, Ltd., Edmonton, Alberta. Anti-sialyl Lewis x (mouse monoclonal IgM, HPLC purified from ascites) and anti-sialyl Lewis a (mouse monoclonal IgG3, ammonium sulfate precipitate of ascites) antibodies (31–33) were provided by Dr. Paul Terasaki (University of California, Los Angeles, CA). Fluorescein isothiocyanate-conjugated goat anti-mouse IgM or IgG antibodies were purchased from Sigma.

Murine Genomic Library Screening—Approximately 1.0×10^6 recombinant λ phage from a genomic library prepared from mouse 3T3 cell DNA (Stratagene) were screened by plaque hybridization, as described previously (35). Phage lifts were prepared with nitrocellulose filters (Schleicher and Schuell). Filters were prehybridized at 32 °C for 2 h in 50% formamide, 5 × standard saline citrate (SSC), 1 × PE (1 × PE is 50 mM Tris, ph 7.5, 0.1% sodium pyrophosphate, 1% sodium dodecyl sulfate, 0.2% polyvinylpyrolidone (M_r 40,000), 0.2% Ficoll (M_r 40,000), and 5 mM EDTA). (35), and 150 mg/ml sheared salmon sperm DNA. Filters were sequentially hybridized at 32 °C for 16 h in prehybridization solution containing a ^{32}P-labeled (36) probe consisting of a 468-bp *Ava*I-*Pvu*II human Fuc-TIV fragment. Alternatively, filters were screened with a 324-bp probe derived from bp 571 to bp 894 of the human Fuc-TIII cDNA (37). After hybridization, filters were rinsed twice for 15 min each at room temperature in 2 × SSC, 0.5% sodium dodecyl sulfate; once for 30 min at 55 °C in 2 × SSC, 0.5% SDS; and then subjected to autoradiography. 11 independent hybridization-positive plaques were isolated after two additional cycles of screening with the human Fuc-TIV fragment. In the subsequent cycles, filters were subjected to an additional final rinse of 30 min at 65 °C, in 0.1 × SSC, 0.1% SDS. Phage DNAs were prepared from liquid lysates (38) and were subsequently characterized by restriction endonuclease digestions, Southern blot analyses, and sequencing.

Subcloning and DNA Sequence Analysis—A 1.4-kb *Nco*I-*Ssp*I fragment homologous to the human FucT-IV probe (468-bp *Ava*I-*Pvu*II fragment, Ref. 20) was isolated from the phage DNA and subcloned into pTZ19R plasmid vector. A 2.6-kb *Sac*I fragment homologous to the human Fuc-TIII probe (representing the murine α1–3FT pseudogene described under "Results") was isolated from phage DNA and subcloned into the *Sac*I site of pTZ19R. The DNA sequences of these fragments were determined by dideoxy method using Sequenase sequencing kit (U. S. Biochemical Corp.). Sequence analysis was performed using the sequence analysis software package (GCG) of the University of Wisconsin Genetics Computer Group (39) and the MacVector version of the IBI Pustell Sequence Analysis Software package (International Biotechnologies, Inc.). Sequence alignments were assembled with the GAP and BESTFIT functions of the GCG package.

Northern Blot Analysis—Total RNA was prepared from mouse (FVB strain) tissues and cultured cells, using procedures described previously (38). Poly(A)$^+$ RNA was isolated with oligo(dT)-cellulose (Collaborative Research) chromatography (38). RNA samples were electrophoresed through 1.0% agarose gels containing formaldehyde (38) and were transferred to a nylon membrane (Hybond-N, Amersham Corp.). Northern blots were prehybridized for 2 h at 42 °C in 1 × PE (35), 5 × SSC, 0.5% sodium dodecyl sulfate, and 150 μg/ml sheared salmon sperm DNA. Blots were hybridized for 18 h at 42 °C in prehybridization solution containing a ^{32}P-labeled (36) 1.4-kb *Nco*I-*Ssp*I fragment. This sequence begins at the most proximal putative initiation codon shown in Fig. 1 and ends at an *Ssp*I site approximately 90 bp distal to the termination codon. Blots were stripped in boiling 0.1% SDS and rehybridized with a β-actin probe to confirm that RNA samples were intact and loaded in equivalent amounts.

Transfection and Expression of Murine Fuc-TIV Gene—The 1.4-kb *Nco*I-*Ssp*I fragment was subcloned into the plasmid pcDNAI. A plasmid containing a single insert in the sense orientation relative to the plasmid's cytomegalovirus promoter-enhancer sequences was designated pcDNAI-mFuc-TIV. COS-7 cells were transfected with this plasmid, with the control plasmid pcDNAI, or with pcDNAI-hFuc-TIV (20), using a DEAE-dextran procedure (38) as described previously (37, 40). A 1.8-kb *Hpa*I-*Xba*I fragment derived from the murine putative pseudogene was cloned between the *Eco*RV and *Xba*I sites in the mammalian expression plasmid pcDNAI. A plasmid containing a single insert in the sense orientation was designated pcDNAI-MPFT.

Flow Cytometry Analysis—COS-7 cells transfected with plasmid pcDNAI-mFuc-TIV were harvested (40) 72 h after transfection and stained with monoclonal antibodies diluted in staining media, as described previously (37, 40). Anti-Lewis a, anti-H, and anti-sialyl Lewis x antibodies (mouse IgM) were used at 10 μg/ml. Anti-Lewis x antibody (mouse IgM anti-SSEA-1; ascites) was used at a dilution of 1:1000. Anti-sialyl Lewis a (mouse IgG; ascites) was used at a dilution of 1:500. Cells were then stained with fluorescein isothiocyanate-conjugated goat anti-mouse IgM or anti-mouse IgG and subjected to analysis on a FACScan (Becton Dickinson) as described previously (37). Thresholds for antigen positivity were set at a fluorescence intensity level that excludes 99% of transfected COS-7 cells that had been stained with the test antibody (anti-H).

α1–3FT Assays—Cell extracts containing 1% Triton X-100, 25% glycerol were prepared from transfected COS-7 cells using procedures described previously (37). α1–3FT assays were performed in a total volume of 20 μl. In preliminary experiments designed to optimize the conditions for activity determination, the reaction mixture contained 3 μM GDP-[^{14}C]fucose, 20 mM acceptor (*N*-acetyllactosamine), and a quantity of cell extract protein sufficient to yield linear reaction conditions. Neutral acceptors were purchased from Sigma (*N*-acetyllactosamine, lactose, lacto-*N*-biose I, 2′-fucosyllactose) or from V-labs (Galα1–3Galβ1–4GlcNAc). The reaction mixture utilized for kinetic calculations included 50 mM Tris-HCl buffer, pH 6.8, 5 mM ATP, 10 mM L-fucose, 5 mM $MnCl_2$, 3 μM GDP-[^{14}C]fucose, and 0.5–1.5 μg of protein extract. Concentrations of acceptor substrates, or GDP-fucose, were varied as indicated in the legends to Figs. 3, 4, and 5. Synthesis and characterization of unlabeled GDP-fucose utilized for GDP-fucose concentration activity determinations has been described previously (41). The concentrations of GDP-fucose in stock solutions were calculated from the UV absorbance at 254 nm of an aliquot diluted in water. The molar extinction coefficient of GDP (ϵ = 13,800 at 254 nm, pH 7.0, Ref. 42) was used for this calculation since the extinction coefficient of GDP-fucose is not available. Reactions were incubated at 37 °C for 1 h. Blanks were prepared by omitting the acceptor in the reaction mixture, and their values were subtracted from the corresponding reaction that

contained acceptor. This background radioactivity reproducibly represented less than 1% of the total radioactivity in the assays and corresponds to the [^{14}C]fucose present in the GDP-[^{14}C]fucose as obtained from the manufacturer.

Reactions containing neutral acceptors (*N*-acetyllactosamine, lactose, lacto-*N*-biose I, 2′-fucosyllactose, Galα1–3Galβ1–4GlcNAc) were terminated by the addition of 20 μl of ethanol and 560 μl of water. Samples were centrifuged at 15,000 $\times$ *g* for 5 min, and a 50-μl aliquot was subjected to scintillation counting to determine the total amount of radioactivity in the reaction. An aliquot of 200 μl was applied to a column containing 400 μl of Dowex 1-X2–400, formate form (35, 37). The column was washed with 2 ml of water, and the radioactive reaction product, not retained by the column, was quantitated by scintillation counting. Reactions with the acceptor α-(2–3)-sialyl-*N*-acetyllactosamine were terminated by adding 980 μl of 5.0 mM sodium phosphate buffer, pH 6.8. Samples were then centrifuged at 15,000 $\times$ *g* for 5 min, and a 500-μl aliquot was applied onto a Dowex 1-X8–200 column (1 ml) prepared in the phosphate form. The reaction product was collected in the eluate and quantitated as described previously (43).

The structure of the product obtained with α-(2–3)-sialyl-*N*-acetyllactosamine was confirmed by HPLC fractionation, before and after neuraminidase digestion, as described previously (20). The structures of the products obtained with the neutral acceptor substrates (*N*-acetyllactosamine, lactose, lacto-*N*-biose I, 2′-fucosyllactose) were also confirmed by HPLC fractionation, using methods described previously (20, 37, 44, 45). The structure of the radiolabeled product (Galα1–3Galβ1–4([^{14}C]Fucα1–3)GlcNAc) obtained with the neutral trisaccharide Galα1–3Galβ1–4GlcNAc was confirmed in separate experiments, using methods described previously (20, 37). The product was purified by chromatography on Dowex 1-X2–400, formate form (35, 37), and subsequently fractionated by amine absorption HPLC (Dynamax 60A column, Rainin Instruments; isocratic gradient in 70% acetonitrile, 30% water; flow rate of 1 ml/min) (37, 44, 45). This product was identified as a tetrasaccharide by virtue of co-elution, at 19 min, with a radiolabeled trisaccharide standard (Fucα(1–2)Galβ1–4([^{14}C]Fucα1–3)GlcNAc). The tetrasaccharide product was digested with 0.01 units of jack bean α-galactosidase (Boehringer Mannheim) for 1 h at 37 °C in 100 mM Tris, pH 6.5. The digest was desalted by Dowex chromatography and fractionated by HPLC exactly as described above for the product. The product of this digestion was identified as a trisaccharide by virtue of co-elution, at 13.4 min, with the trisaccharide standard (Galβ1–4([^{14}C]Fucα1–3)GlcNAc.

In Situ Hybridization Analysis—A segment of the murine Fuc-TIV gene encompassing nucleotide positions 270–756 was amplified by the polymerase chain reaction and subcloned into plasmid vector pcDNAI (Clontech). Antisense or sense RNA *in situ* hybridization probes were generated using this plasmid as a template in Sp6 or T7 RNA polymerase-directed *in vitro* transcription mixtures containing α-[^{35}S]UTP (Amersham Corp.). Probe lengths were adjusted to an average of 250 nucleotides by limited alkaline hydrolysis. Alternatively, antisense or sense RNA *in situ* hybridization probes were generated in a similar manner, were derived from a segment of the murine Fuc-TIV gene encompassing nucleotide positions 491–746, and were used directly without prior alkaline hydrolysis.

Cryosections (10 μm thick) were prepared with Jung Frigocut 2800N cryostat (Leica) from organs of 129/J strain mice. Tissue sections were fixed in 4% paraformaldehyde/phosphate-buffered saline for 30 min at room temperature. After proteinase K treatment and then acetylation by acetic anhydride, sections were incubated with antisense or sense probes (2×10^4 cpm/μl) for 18 h at 55 °C in 20 mM Tris-HCL, pH 8.0, 300 mM NaCl, 5 mM EDTA, 10 mM sodium pyrophosphate, 50% formamide, 10% dextran sulfate, 5 $\times$ Denhardt's solution, 50 mg/ml heparin, 0.1 M dithiothreitol, and 0.5 mg/ml *Escherichia coli* tRNA. The slides were washed for 30 min at 65 °C in 50% formamide, 2 $\times$ SSC, 10 mM dithiothreitol. The sections were then subjected to digestion with 10 μg/ml of ribonuclease A at 37 °C to eliminate residual nonbase-paired probe and were then washed again in the wash solution described above. Slides were exposed for 2 weeks using Kodak NBT-2 emulsion and processed using D-19 developer and fixer (Eastman Kodak Co.). The sections were subsequently stained with hematoxylin and eosin.

Interspecific Mouse Backcross Mapping—Interspecific backcross progeny were generated by mating (C57BL/6J $\times$ *Mus spretus*) F_1 females and C57BL/6J males as described previously (46). A total of 205 N_2 mice were used to map the *Fut*4 locus (see "Results" for details). DNA isolation, restriction enzyme digestion, agarose gel electrophoresis, Southern blot transfer, and hybridization were performed essentially as described previously (47). All blots were prepared with Hybond-N$^+$ nylon membrane (Amersham Corp.). A probe corresponding to base pairs 172-1203 (see Fig. 1) of the mouse Fuc-TIV coding region was labeled with [α-^{32}P]dCTP using a nick translation labeling kit (Boehringer Mannheim); washing was done to a final stringency of 1.0 $\times$ SSC, 0.1% SDS, 65 °C. A fragment of 5.8 kb was detected in *Hin*dIII-digested C57BL/6J DNA, and a fragment of 4.7 kb was detected in *Hin*dIII-digested *M. spetus* DNA. The presence or absence of the 4.7-kb *M. spretus*-specific *Hin*dIII fragment was followed in backcross mice.

A description of the probes and RFLPs for the loci linked to *Fut4* including murine macrophage metalloelastase (*Mmel*), low density lipoprotein receptor (*Ldlr*), and erythropoietin receptor (*Epor*) has been reported previously (48). Recombination distances were calculated as described previously (49) using the computer program SPRETUS MADNESS. Gene order was determined by minimizing the number of recombination events required to explain the allele distribution patterns.

RESULTS

Molecular Cloning of a Murine α1–3FT Gene—A hybridization screen for a murine α1–3FT gene (see "Experimental Procedures") yielded numerous phages that cross-hybridize with probes derived from human α1–3FT genes. Sequence analysis of the insert in a representative of a group of phages with similar restriction maps identified a region with a substantial amount of primary sequence similarity to the coding portion of the human Fuc-TIII gene (62% sequence identity; data not shown; sequence deposited in GenBank, accession number U33458). However, translation of this murine sequence to maintain primary amino acid sequence similarity to Fuc-TIII required the conceptual suppression of multiple frameshift and nonsense mutations in the murine sequence. Furthermore, this sequence did not yield detectable α1–3FT activity when expressed in COS-7 cells (data not shown). These observations indicate that this murine sequence represents a pseudogene; this sequence was not further analyzed.

This hybridization screen also identified phages containing a 1.4-kb *Nco*I-*Ssp*I fragment that cross-hybridizes with the human α1–3FT gene encoding Fuc-TIV (19–21). Sequence analysis of the gene fragment identifies a single long open reading frame (Fig. 1), which begins with a methionine codon located within a sequence context largely consistent with Kozak's consensus rules for mammalian translation initiation (52). Hydropathy analysis (53) of the protein sequence predicted by this open reading frame identifies a single 22-amino acid hydrophobic segment at the NH_2 terminus, implying that the polypeptide has a type II transmembrane topology typical of mammalian glycosyltransferases (16, 54). Sequence comparisons made between the predicted murine protein and human α1–3FTs identify significant primary sequence similarities; the murine protein maintains approximately 33, 33, 39, and 37% amino acid sequence identity with the human Fuc-TIII (37), Fuc-TVI (45), Fuc-TVII (55, 56), and Fuc-TV (57) enzymes, respectively (data not shown). However, it is most similar to human Fuc-TIV (19–21), which shares 77% amino acid sequence identity with the murine protein (304 identities at 396 aligned residues; Fig. 1). This sequence similarity includes the conservation of two consensus sites for asparagine-linked glycosylation (Fig. 1).

Maximal sequence similarity is achieved by aligning the murine DNA sequence in a colinear manner with the sequence of the human Fuc-TIV gene (19, 20) and its cDNA (21). Like the human Fuc-TIV/ELFT locus, the murine gene apparently maintains a single coding exon. Primer extension experiments and RNase protection analyses designed to define the transcriptional initiation site for this murine gene have failed because of the tendency for its transcript to form secondary structure that is resistant to denaturation (data not shown). This is most probably a function, in part, of the extraordinarily high G+C content within the 5′ end of this gene. We also believe these observations explain our inability to isolate full-length murine Fuc-TIV cDNAs from multiply screened high quality cDNA libraries (data not shown). Nonetheless, comparison of

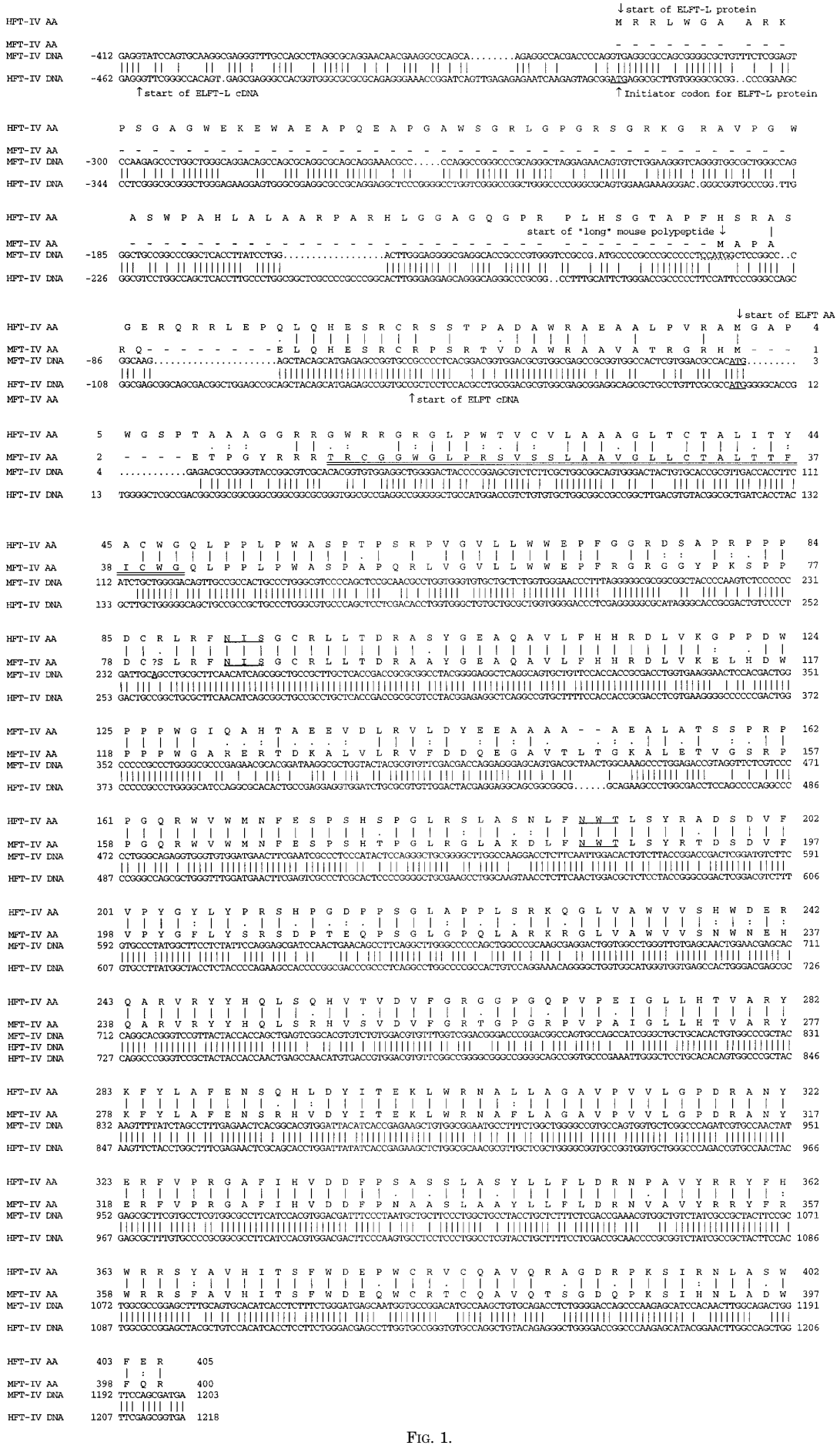
↓start of ELFT-L protein
↑start of ELFT-L cDNA
↑Initiator codon for ELFT-L protein
start of "long" mouse polypeptide ↓
↓start of ELFT AA
↑start of ELFT cDNA

FIG. 1.

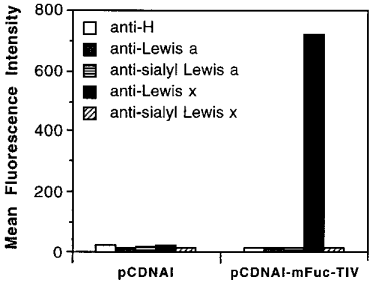

FIG. 2. **Flow cytometry histograms of COS-7 cells transfected with the murine Fuc-TIV gene.** Cells transfected with either the α1–3FT expression vector pcDNAI-mFuc-TIV or the control vector pcDNAI were stained with the monoclonal antibodies indicated in the *inset* and were subjected to flow cytometry analysis ("Experimental Procedures"). The data presented are the mean (linear) fluorescence intensities of the antigen-positive population of transfected cells (see "Experimental Procedures").

the DNA sequences of the murine and human genes through positions exceeding 400 base pairs proximal to their respective initiation codons discloses that their respective 5′-flanking regions are identical at 66% of the aligned positions (Fig. 1). This high level of DNA sequence identity is maintained throughout the region of the human gene where it is co-linear with Fuc-TIV/ELFT mRNA transcripts (Fig. 1), as defined by cDNA cloning experiments (21), which in turn yield Fuc-TIV/ELFT or a longer form of this enzyme (ELFT-L; Ref. 21). The murine gene also has the potential to yield a longer form of its polypeptide product. This longer sequence is represented by a polypeptide initiating at a methionine codon located 33 codons 5′ to the human Fuc-TIV/ELFT initiator methionine codon, extending the shorter murine polypeptide by 33 amino acid residues at its NH_2 terminus (Fig. 1). This longer murine sequence maintains 52% amino acid sequence identity with the ELFT-L polypeptide in a region immediately proximal to the Fuc-TIV/ELFT initiator methionine residue (Fig. 1). These observations further support the conclusion that the murine gene maintains a structural organization essentially identical to that of the human Fuc-TIV/ELFT gene.

Expression of the Mouse α1–3FT Gene in COS-7 Cells—To confirm that this murine sequence encodes a functional α1–3FT, the 1.4-kb *Nco*I-*Ssp*I fragment encompassing the open reading frame was cloned into the mammalian expression vector pcDNAI (see "Experimental Procedures"), and the resulting plasmid (pcDNAI-mFuc-TIV) was introduced into COS-7 cells by transfection. COS-7 cells transfected with pcDNAI-mFuc-TIV were analyzed by flow cytometry to assess the intracellular acceptor substrate requirements of the murine enzyme (Fig. 2). COS-7 cells are appropriate hosts for these experiments since they express neutral and α-(2–3)-sialylated oligosaccharide precursors used by α1–3FTs to construct surface-localized Lewis x (Galβ1–4[Fucα1–3]GlcNAc), sialyl Lewis x, (NeuAcα2–3Galβ1–4[Fucα1–3]GlcNAc), Lewis a (Galβ1–3[Fucα1–4]GlcNAc), and sialyl Lewis a (NeuAcα2–3Galβ1–3[Fucα1–4]GlcNAc) determinants (45, 55). These analyses demonstrate that pcDNAI-mFuc-TIV can determine surface expression of the Lewis x determinant, but not the sialyl Lewis x, sialyl Lewis a, or Lewis a structures (Fig. 2). These results are virtually identical to those obtained with the human Fuc-TIV gene (19, 20, 55).

In Vitro Enzyme Assay of Mouse and Human Fuc-TIVs—COS-7 cells transfected with pcDNAI-mFuc-TIV also contain a substantial amount of α1–3FT activity that utilizes the acceptor *N*-acetyllactosamine. This murine enzyme has a pH optimum of 7.5 (Fig. 3) and is maximally stimulated by Mn^{2+} (5-fold) at a concentration of 15 mM (Fig. 3). In comparison, the human Fuc-TIV enzyme (20) is optimally active at pH 7.3 and is maximally stimulated by Mn^{2+} (4-fold) at a concentration of 10 mM, when assayed with *N*-acetyllactosamine (Fig. 3).

Kinetic analyses of murine and human Fuc-TIV enzymes indicate that they exhibit typical substrate concentration-dependent Michaelis-Menten kinetics (Figs. 4 and 5). The calculated apparent Michaelis constants for the donor substrate GDP-fucose are 16.6 and 27.0 μM for the murine and human enzymes, respectively (Fig. 4). The apparent Michaelis constants for the acceptor substrates *N*-acetyllactosamine and α-(2–3)-sialyl-*N*-acetyllactosamine are 2.05 and 1.78 mM, respectively, for the murine enzyme, and 3.3 mM and 6.74 mM, respectively, for human Fuc-TIV (Fig. 5). Both enzymes utilize the neutral type II acceptor molecules 2′-fucosyllactose and lactose with efficiencies that are substantially less than those obtained with either α-(2–3)-sialyl-*N*-acetyllactosamine or *N*-acetyllactosamine. For example, a single preparation of the murine enzyme utilized 2′-fucosyllactose and lactose at rates that were 7% (1.1 nmol/mg·h) and 1% (0.2 nmol/mg·h), respectively, of the rate obtained with *N*-acetyllactosamine (16.6 nmol/mg·h). Only trace amounts of fucosylated product were produced when the neutral type I acceptor lacto-*N*-biose I was assayed with the same preparation of murine enzyme (0.05 nmol/mg·h). These results are virtually identical to those obtained when extracts containing human Fuc-TIV activity are assayed with the latter three substrates (20, 55). Thus, when considered together with the DNA and protein sequence comparisons and the flow cytometry analyses, these biochemical data indicate that the open reading frame shown in Fig. 1 encodes an α1–3FT activity that corresponds to a human "myeloid"-type α1–3FT (Fuc-TIV/ELFT) (19–21, 58, 59).

The Galα1–3Galβ1–4GlcNAc trisaccharide is a cell surface oligosaccharide epitope expressed by many murine tissues (60). There is indirect evidence for a fucosylated form of this epitope

FIG. 1. **Nucleotide and deduced amino acid sequences of the murine α1–3FT gene and comparison to the human Fuc-TIV/ELFT gene and its cDNAs.** The DNA sequence of the murine gene, and its predicted protein sequences, correspond to *MFT-IV DNA*, and *MFT-IV AA*, respectively. The DNA sequence of the human Fuc-TIV/ELFT gene, and predicted protein sequences, correspond to lines denoted by *HFT-IV DNA*, and *HFT-IV AA*, respectively. The A residues of the putative initiation codon of the murine α1–3FT gene and of the human ELFT/Fuc-TIV sequence are assigned as residue 1 of their nucleotide sequence. The methionine residues corresponding to these codons are assigned as residue 1 of the corresponding protein sequences. These positions are further denoted by an *arrow* pointing to these aligned initiator methionine codons (*start of ELFT AA*). The initiation codon for the "long" form of ELFT (21) is also indicated by *arrows* (*start of ELFT AA*; *Initiator codon for ELFT-L protein*). The initiator methionine for the long form of the murine polypeptide is also indicated by an *arrow* (*start of "long" mouse polypeptide*). This methionine codon is encompassed within the *Nco*I site (*dotted underlined*) used to construct the vector pcDNAI-mFuc-TIV. *Arrows* also indicate the 5′-most residues found in the ELFT and ELFT-L cDNAs (21) (*start of ELFT cDNA*; *start of ELFT-L cDNA*). The sequence alignment was generated using the BESTFIT and GAP programs of the University of Wisconsin Genetics Computer Group (39). The GAP program generates symbols between aligned amino acids, according to the evolutionary distance between them, as measured by Dayhoff (50) and normalized by Gribskov (51). Amino acid sequence identities are assigned a score of 1.5, denoted by a *vertical bar*; related amino acid residues with scores from 0.5 to 1.4 are denoted by a *two dots*, less strongly related amino acid residues with scores between 0.1 to 0.4 are denoted by *one dot*; no symbol is placed between dissimilar amino acid pairs with scores less than 0.1. Gaps in the amino acid sequence alignment are denoted by a *dash*. Nucleotide sequence identity is indicated by *vertical lines* between aligned corresponding residues. Gaps in the nucleotide sequence alignment are indicated by a *dotted line*. The predicted transmembrane domain of the murine enzyme (amino acids 53–74) is *double underlined*. Consensus sites for asparagine-linked glycosylation are *underlined*.

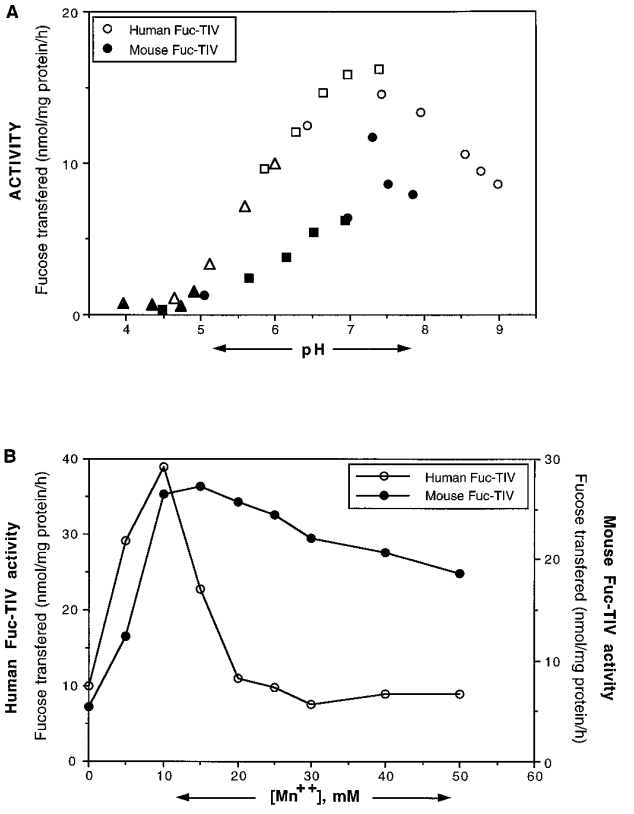

FIG. 3. **pH- and Mn^{2+} concentration-α1–3FT activity profiles.** *A*, pH-activity profiles. The enzymatic activity in COS-7 cells transfected with pcDNAI-mFuc-TIV or pcDNAI-hFuc-TIV (20) was assayed using 20 mM *N*-acetyllactosamine and 3 mM GDP-[^{14}C]fucose (see "Experimental Procedures"). Reactions contained 50 mM sodium acetate, ■; sodium phosphate, ●; or Tris-HCl, ▲. *B*, Mn^{2+} concentration-activity profiles. The enzymatic activity in COS-7 cells transfected with pcDNAI-mFuc-TIV or pcDNAI-hFuc-TIV was assayed using 20 mM *N*-acetyllactosamine and 3 μM GDP-[^{14}C]fucose ("Experimental Procedures"). Reactions contained 50 mM Tris-HCl, pH 7.2.

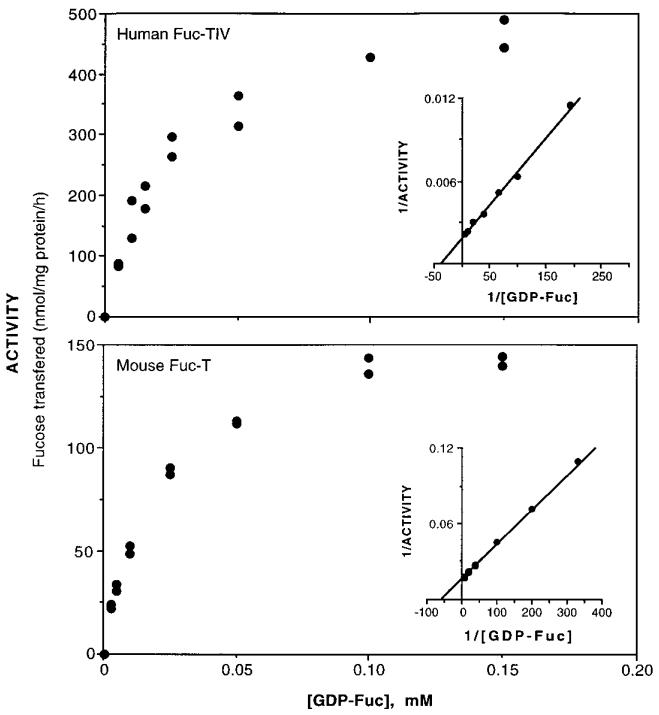

FIG. 4. **Apparent Michaelis constants for GDP-[^{14}C]fucose determined for mouse and human Fuc-TIVs.** Apparent K_m values were determined (see "Experimental Procedures") in the presence of 20 mM *N*-acetyllactosamine, 15 mM Mn^{2+}, and 50 mM Tris-HCl, pH 7.2. Cell extracts prepared from COS-7 cells transfected with pcDNAI-mFuc-TIV exhibited an apparent K_m of 16.6 μM, whereas human Fuc-TIV extracts generated using plasmid pcDNAI-hFuc-TIV maintained an apparent K_m of 27.0 μM.

in murine tissues (Galα1–3Galβ1–4[Fucα1–3]GlcNAc; Ref. 10). *In vitro* studies using a human α1–3FT suggest that fucosylation can be a terminal step in the synthesis of this tetrasaccharide (61). We find that the murine α1–3FT can efficiently utilize the trisaccharide Galα1–3Galβ1–4GlcNAc (with an apparent K_m = 0.71 mM; Fig. 5*C*) to form a fucosylated product corresponding to the tetrasaccharide Galα1–3Galβ1–4[Fucα1–3]GlcNAc (see "Experimental Procedures"). This observation suggests that murine glycoconjugates containing the Galα1–3Galβ1–4GlcNAc trisaccharide represent one authentic acceptor substrate for this murine α1–3FT. Although the human Fuc-TIV enzyme can also form this tetrasaccharide product *in vitro* (data not shown), this reaction has no apparent physiological relevance since the human genome does not encode a functional α(1–3)-galactosyltransferase capable of synthesizing Galα1–3Galβ1–4GlcNAc precursors(62).

Chromosomal Location of the Murine α1–3FT Locus—The mouse chromosomal location of this Fuc-TIV-like gene (locus designation *Fut4*) was determined by interspecific backcross analysis using progeny derived from matings of ((C57BL/6J × *M. spretus*)F_1 × C57BL/6J) mice. This interspecific backcross mapping panel has been typed for over 1600 loci that are well distributed among all of the autosomes as well as the X chromosome (46). C57BL/6J and *M. spretus* DNAs were digested with several enzymes and analyzed by Southern blot hybridization for informative restriction fragment length polymorphisms using a mouse Fuc-TIV probe (see "Experimental Procedures"). The 4.7-kb *M. spretus Hin*dIII restriction fragment-length polymorphism ("Experimental Procedures") was used to follow the segregation of the *Fut4* locus in backcross mice. The mapping results indicated that *Fut4* is located in the proximal region of mouse chromosome 9 linked to *Mmel*, *Ldlr*, and *Epor*. Although 138 mice were analyzed for every marker and are shown in the segregation analysis (Fig. 6), up to 173 mice were typed for some pairs of markers. Each locus was analyzed in pairwise combinations for recombination frequencies using the additional data. The ratios of the total number of mice exhibiting recombinant chromosomes to the total number of mice analyzed for each pair of loci and the most likely gene order are as follows: centromere - *Mmel* - 3/173 - *Fut4* - 4/150 - *Ldlr* - 1/161 - *Epor*. The recombination frequencies (expressed as genetic distances in centimorgans ± the standard error) are as follows: - *Mmel* - 1.7 ± 1.0 - *Fut4* - 2.7 ± 1.3 - *Ldlr* - 0.6 ± 0.6 - *Epor*.

The proximal region of mouse chromosome 9 shares a region of homology with human chromosomes 11q and 19p (summarized in Fig. 6). The human Fuc-TIV gene (locus designation *FUT4*) was initially assigned to human 11q12-qter (63). More recently, the human map position has been refined to 11q21 (64). These studies provide additional support for concluding that this murine gene is the human homologue of Fuc-TIV gene, and confirm and extend the region of homology between mouse chromosome 9 and the long arm of human chromosome 11.

Tissue-specific Expression of the Murine Fuc-TIV Gene—Northern blot analyses were completed to define the tissue-specific expression patterns of this murine α1–3FT gene. A single transcript, approximately 4.4 kb in length, was detected on blots prepared with polyadenylated RNA isolated from various murine tissues and blood-derived cell lines (Fig. 7). This transcript is most abundant in the stomach and colon; substan-

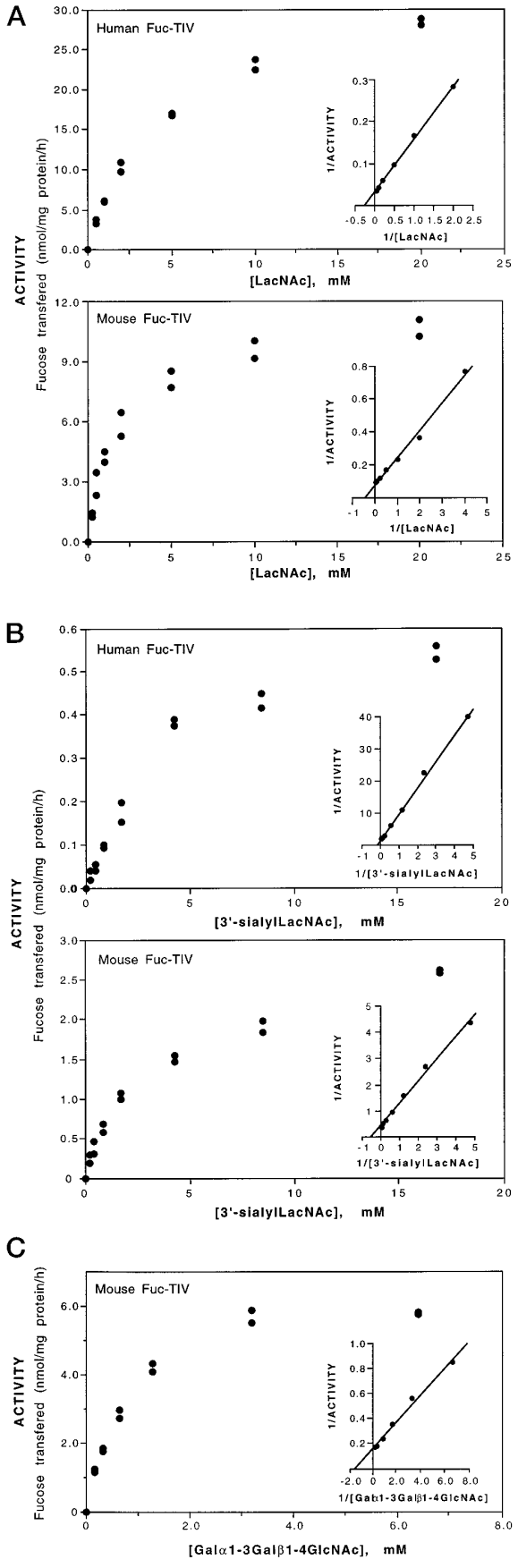

FIG. 5. **Apparent Michaelis constants for *N*-acetyllactosamine and α-(2–3)-sialyl-*N*-acetyllactosamine, determined for murine and human Fuc-TIVs.** Apparent K_m values were determined (see "Experimental Procedures") in the presence of 3 μM GDP-fucose, 15 mM Mn^{2+}, and 50 mM Tris-HCl, pH 7.2. *A*, *N*-acetyllactosamine K_m. Using *N*-acetyllactosamine as the acceptor, cell extracts prepared from COS-7 cells transfected with pcDNAI-mFuc-TIV exhibited an apparent K_m of 2.05 mM, whereas human Fuc-TIV extracts generated using plasmid pcDNAI-hFuc-TIV exhibited an apparent K_m of 3.82 mM. *B*, 2′-sialyl-*N*-acetyllactosamine K_m. Apparent K_m values using α-(2–3)-sialyl-*N*-acetyllactosamine as the acceptor were 1.78 mM and 6.74 mM for the murine and human Fuc-TIVs, respectively. *C*, Galα1–3Galβ1–4GlcNAc K_m. The apparent K_m value using Galα1–3Galβ1–4GlcNAc as the acceptor was 0.71 mM for murine Fuc-TIV/ELFT.

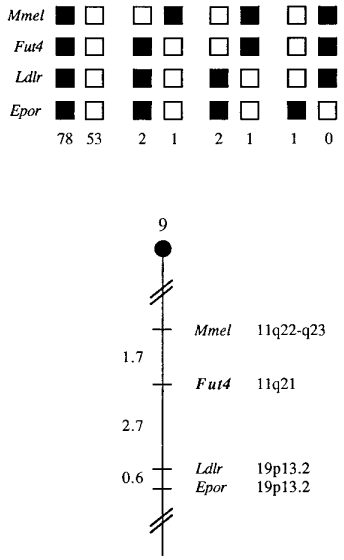

FIG. 6. **Fut4 maps in the proximal region of mouse chromosome 9.** *Fut4* was placed on mouse chromosome 9 by interspecific backcross analysis. The segregation patterns of *Fut4* and flanking genes in 138 backcross animals that were typed for all loci are shown at the *top* of the figure. For individual pairs of loci, more than 138 animals were typed (see text for details). Each column represents the chromosome identified in the backcross progeny that was inherited from the (C57BL/6J × *M. spretus*)F_1 parent. The *shaded boxes* represent the presence of a C57BL/6J allele, and *white boxes* represent the presence of *M. spretus* allele. The number of offspring inheriting each type of chromosome is listed at the *bottom* of each column. A partial chromosome 9 linkage map showing the location of *Fut4* in relation to linked genes is shown at the *bottom* of the figure. Recombination distances between loci in centimorgans are shown to the *left* of the chromosome, and the positions of loci in human chromosomes are shown to the *right*. References for the human map positions of loci cited in this study can be obtained from the Genome Data Base, a computerized database of human linkage information maintained by The William H. Welch Medical Library of The Johns Hopkins University (Baltimore, MD).

tial amounts are also detected in the lung, testes, uterus, and small intestine. Lesser amounts of the Fuc-TIV mRNA are detected in the thymus, spleen, and ovary, and only trace amounts are observed in the brain, heart, smooth muscle, kidney, thymus, and bone marrow. The murine Fuc-TIV transcript is not found in liver, salivary gland, or pancreas at levels detectable by Northern blot analysis using up to 3 μg of polyadenylated mRNA (Fig. 7).

Northern blot analysis of cultured blood cell-type cell lines indicates that the Fuc-TIV transcript is relatively abundant in the murine erythroleukemia cell line MEL (26, 27), substantially less abundant in the RAW macrophage-derived line (28, 29), and not detectable in the P388 macrophage-derived cell line (30) or the three lymphoid cell lines we examined (T-cell line EL4, Ref. 23; mature B-cell lines (hybridomas) S107, Ref. 22; TH2.54.63, Ref. 24; and 180.1, Ref. 25). These results suggest that the murine Fuc-TIV gene, like its human counterpart, may be expressed in cells derived from the myeloid lineage but not in abundance in cells of the lymphoid lineage.

In situ hybridization analysis was used to delineate the cell

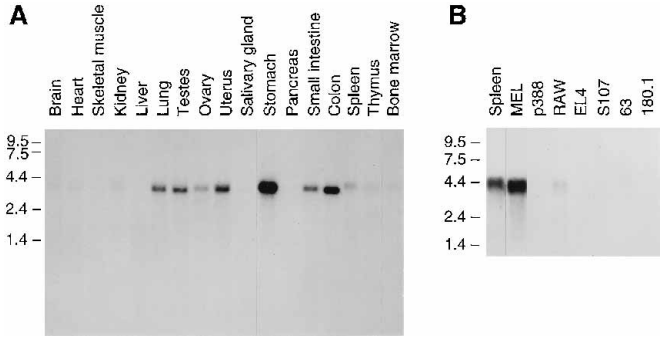

FIG. 7. **Tissue-specific expression patterns of the murine Fuc-TIV gene.** Polyadenylated RNA samples (3 μg) prepared from various murine tissues (*panel A*) and cell lines (*panel B*) were subjected to Northern blot analysis as described under "Experimental Procedures." The blot was probed with the *Nco*I-*Ssp*I fragment using hybridization and wash conditions detailed under "Experimental Procedures." Cell lines represent the following lineages: *MEL*, murine erythroleukemia cell line; *P388* and *RAW* (RAW 264.7), macrophage; *EL4*, T-cell; *S107*, *63* (TH2.54.63), and *180.1*, B-cell lines (hybridomas). RNA molecular size standards, in kb, are indicated at the *left*.

types within some of the organs where relatively abundant levels of this transcript are present (Fig. 8). These experiments demonstrate that the Fuc-TIV transcript accumulates to substantial levels within the epithelial cells lining the stomach and colon (Fig. 8). The Fuc-TIV transcript accumulates to a lesser degree within the epithelial cells (both absorptive cells and goblet cells) lining the small intestinal villi, and the mucus glands within the small intestine. Fuc-TIV transcripts are also evident in the epithelial cells lining the epididymus (Fig. 8) but are not visible within the testis proper (data not shown). These observations correspond well with Fuc-TIV transcript abundance seen on the Northern blot analyses (Fig. 7). No Fuc-TIV transcripts are detected in the kidney or the lung by *in situ* hybridization (data not shown), even though low to moderate levels of the Fuc-TIV transcript are evident on Northern blot analysis. It remains to be determined if this apparent discrepancy may be accounted for by the relatively insensitive nature of the *in situ* hybridization method and/or by Fuc-TIV transcripts in blood cells within the larger vessels of these organs. These cells may contribute to the Northern blot signals but may be eliminated from the tissues prior to or during preparation for *in situ* hybridization. Fuc-TIV transcripts are not detected in murine neutrophils (data not shown); we have yet to define which blood cell lineages, and which maturation stage(s) of those lineages, are responsible for the Fuc-TIV transcripts observed in bone marrow mRNA.

DISCUSSION

Biochemical studies indicate that selectin ligand expression in myeloid and lymphoid lineages is controlled in part by cell type-specific expression of one or more α1–3FTs and that these enzymes consequently play a pivotal role in the human inflammatory response (5–8). Evidence also suggests that the aberrant expression of these enzymes in malignancy may facilitate the spread of transformed cells via selectin-dependent metastatic processes (5–7, 63–67). The developmentally regulated expression patterns of α-(1–3)-fucosylated oligosaccharides in mammalian embryos (2, 9–12) further imply that these molecules have additional, undefined functions. Given logistical and ethical considerations, the laboratory mouse is a useful system to analyze embryonic and adult α1–3FT gene expression patterns and to perturb these patterns through transgenic and embryonic stem cell approaches.

The polypeptide product of the murine gene described here shares 77% amino acid sequence identity with human Fuc-TIV (19–21). Inter-species sequence comparisons have not previously been made for any α1–3FT sequences; the degree of sequence identity observed is comparable with levels reported for other cross-species comparisons of glycosyltransferase sequences (68–70) and suggest that this murine gene is the orthologous homologue (71) of human Fuc-TIV. This assignment is further supported by their corresponding chromosomal localizations and by the genomic organization of the murine gene and the human Fuc-TIV gene, both of which apparently maintain intronless coding sequences.

Comparison of the catalytic properties of the murine enzyme with those of the human Fuc-TIV enzyme provides additional evidence for their homologous nature. Transfection studies indicate that both enzymes can determine expression of surface-localized Lewis x molecules, but not sialyl Lewis x moieties or products based on type I precursors. The mouse and human enzymes maintain similar affinities for the type II acceptor *N*-acetyllactosamine, *in vitro* (2.05 and 3.3 mM, respectively), but differ somewhat in their apparent affinities for α-(2–3)-sialyl-*N*-acetyllactosamine. Specifically, the human enzyme exhibits a rather higher apparent K_m (6.7 mM) for the sialylated substrate than does the mouse enzyme (1.8 mM). Nevertheless, the murine enzyme does not utilize oligosaccharides terminating with α-(2–3)-sialylated type II chains when it is expressed in the cultured cell lines used here. The apparent discrepancy presented by the ability of Fuc-TIV to utilize α-(2–3)-sialylatedtype II oligosaccharides *in vitro*, but not *in vivo*, may be resolved by considering recent results indicating that Fuc-TIV resides in a Golgi compartment proximal to α-(2–3)-sialyltransferase and thus may not have an opportunity to operate upon such substrates within a cell (72). These observations further emphasize that it is difficult to reliably predict the spectrum of oligosaccharide products that will be constructed in a specific cell lineage by a given glycosyltransferase solely by considering the results obtained from *in vitro* assays using low molecular weight oligosaccharide acceptors. This notion is strongly reinforced by results indicating that the human Fuc-TIV gene can, under some circumstances, determine cell surface sialyl Lewis x expression in transfected cells, and that this outcome is critically dependent upon the glycosylation phenotype of the host cell in which Fuc-TIV is expressed (73). Thus, while it seems likely that the murine Fuc-TIV enzyme creates Fucα1–3GlcNAc linkages in murine tissues, it is not yet possible to predict which murine glycoconjugate acceptors will be utilized by this α1–3FT, and, consequently, we cannot yet predict the cell surface products created by this enzyme.

However, one such molecule may correspond to the terminal oligosaccharide structure Galα1–3Galβ1–4GlcNAc. This determinant is widely expressed in murine tissues (60), and, as we have shown here, is efficiently utilized, *in vitro*, by the murine Fuc-TIV/ELFT enzyme. Prior work has provided indirect evidence for the expression of the α-(1–3)-fucosylated form of this molecule (Galα1–3Galβ1–4[Fucα1–3]GlcNAc) by murine cell surface glycoconjugates during the periimplantation period (10). This tetrasaccharide has also been synthesized *in vitro* by a sequential enzyme-assisted synthetic scheme involving α-(1–3)-galactosylation of *N*-acetyllactosamine to form Galα1–3Galβ1–4GlcNAc, followed by α-(1–3)-fucosylation with an α1–3FT isolated from human milk (61). However, since in some cell types the murine α1–3 galactosyltransferase responsible for synthesis of the Galα1–3Galβ1–4GlcNAc precursor trisaccharide is most probably localized to a Golgi compartment coincident with α-(2–3)-sialyltransferase, and distal to the compartment where Fuc-TIV is located (74), it seems probable that simultaneous expression of the Fuc-TIV and α-(1–3)-galactosyltransferase genes will not necessarily yield expression of

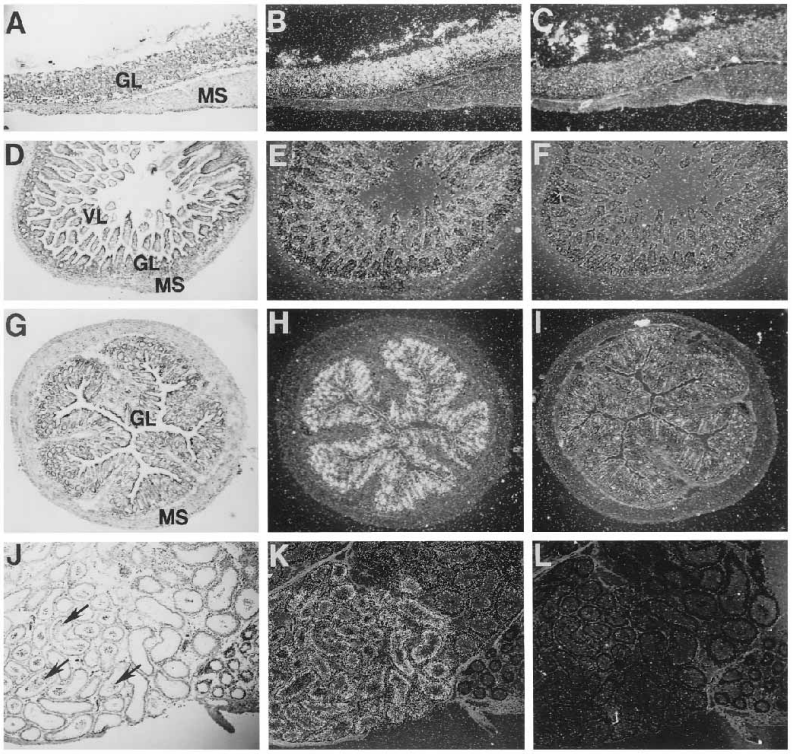

FIG. 8. **In situ hybridization analysis of Fuc-TIV transcripts in murine tissues.** Mouse stomach (*A–C*), small intestine (*D–F*), colon (*G–I*), and epididymus (*J–L*) were hybridized with antisense (*A*, *B*, *D*, *E*, *G*, *H*, *J*, *K*) or sense (*C*, *F*, *I*, *L*) mouse Fuc-TIV probes. *Panels A*, *D*, *G*, and *J* are bright-field photomicrographs, and panels *B*, *C*, *E*, *F*, *H*, and *I* are dark-field photomicrographs, each taken at 40× magnification. *MS*, muscle layer; *GL*, glands; *VL*, villi. *Arrows* in *panel J* point to the tubular lumenae within the epididymus.

this tetrasaccharide. Additional information concerning the expression pattern of this tetrasaccharide will await the development of antibodies directed against this molecule.

The Galα1–3Galβ1–4[Fucα1–3]GlcNAc tetrasaccharide represents a noncharged analogue of the sialyl-Lex determinant, prompting a suggestion that it may represent a possible ligand for the selectins (61). It is not yet known if this tetrasaccharide can participate in selectin-dependent cell adhesion processes or if it is expressed by murine neutrophils, although the precursor trisaccharide determinant is displayed by these cells.[2] It is interesting to note in this context that the oligosaccharide portion of the murine E- and P-selectin counter-receptors are not yet defined, although the sialyl Lewis x determinant is not expressed on murine leukocytes (75), at least as defined by the use of the monoclonal antibody CSLEX. The tissue-specific expression patterns, and functions, if any, of this tetrasaccharide molecule thus remain an open and interesting question.

Northern blot analyses identify a single mouse Fuc-TIV transcript in all tissues where the gene is expressed, whereas the human Fuc-TIV gene generates multiple transcripts (19–21). By analogy to other mammalian glycosyltransferase mRNAs (16, 54), the relatively large size of the mouse Fuc-TIV transcript suggests that it contains substantial amounts of 3′- and/or 5′-untranslated segments. The structure of this transcript remains to be determined by cloning and sequencing of the cDNA(s) derived from this gene. While the murine transcript is detectable in bone marrow, the specific marrow cell types that express this gene remain to be precisely defined. It is likely, however, that the marrow transcripts are derived in part from myeloid-lineage cells since the human Fuc-TIV gene is expressed in myeloid cells (19–21). The murine erythroid lineage may also contribute to expression in the bone marrow since transcripts are detected in the mouse erythroleukemia line MEL. The murine transcript is also relatively abundant in the epithelial cells lining the colon and stomach, with somewhat lesser amounts in small intestinal epithelial cells. The function of this enzyme in these locations remains unknown, although it is interesting to speculate that it serves to participate in the synthesis of fucosylated mucins that may operate to protect the gastrointestinal lining from destructive effects of digestive enzymes or from ingested pathogens. The low levels of the Fuc-TIV transcript in the testes is accounted for by transcripts that accumulate in the epididymus. The low levels of Fuc-TIV message detected in the kidney, and the trace amounts identified in brain and heart, may represent transcripts derived from specific cell types within the parenchyma of these organs. Further *in situ* hybridization experiments will be required to confirm this possibility.

These results indicate that while the murine and human Fuc-TIV genes are similarly organized, there may be substantial interspecies differences in the structural, functional, and regulatory properties of the orthologous α1–3FTs. Evidence suggests that the functional roles of their oligosaccharide products may also differ in significant ways. The expression patterns exhibited by the mouse α1–3FT gene are different from those shown by a rat α-(2–6)-sialyltransferase gene (76, 77), a constitutively expressed mouse β-(1–4)-galactosyltransferase gene (78, 79), a mouse α-(1–3)-galactosyltransferase gene (60), and a series of human sialyltransferase genes (80). When considered together with these data, our results provide additional support for the notion that transcriptional control of glycosyltransferase gene expression regulates cell surface glycosylation (54, 80).

Functional correlates for the regulation of this α1–3FT remain to be explored. In this context, we have compared our interspecific map of chromosome 9 with a composite mouse linkage map that reports the map location of many uncloned mouse mutations.[3] *Fut4* maps in a region of the composite map that lacks mouse mutations with a phenotype that might be expected for an alteration in this locus (data not shown). The task of assigning function to this locus

[2] A. Thall and J. B. Lowe, unpublished data.

[3] Compiled by M. T. Davisson, T. H. Roderick, A. L. Hillyard, and D. P. Doolittle and provided from GBASE, a computerized data base maintained at the Jackson Laboratory, Bar Harbor, ME.

may be facilitated by a more complete understanding of the types, structures, and expression patterns of this and other murine glycosyltransferase genes and their cognate oligosaccharide products, in concert with approaches that utilize transgenic and gene ablation technologies in the mouse.

Acknowledgments—We thank Paul Terasaki for providing the anti-sialyl Lewis x and anti-sialyl Lewis a monoclonal antibodies and Davor Solter for the anti-SSEA-1 antibody. We also thank Sally Camper, Michael Imperiale, Rajan Nair, and Linda Samuelson for useful discussions and David Ginsburg for reviewing this manuscript. We thank B. Cho for excellent technical assistance.

REFERENCES

1. Bird, J. M., and Kimber, S. J. (1984) *Dev. Biol.* **104,** 449–460
2. Fenderson, B. A., Zehavi, U., and Hakomori, S. (1984) *J. Exp. Med.* **160,** 1591–1596
3. Hakomori, S.-I. (1984) *Annu. Rev. Immunol.* **2,** 103–126
4. Varki, A. (1994) *Proc. Natl. Acad. Sci. U. S. A.* **91,** 7390–7397
5. Lowe, J. B., Stoolman, L. M., Nair, R. P., Larsen, R. D., Berhend, T., and Marks, R. M. (1990) *Cell* **63,** 475–484
6. Phillips, M. L., Nudelman, E., Gaeta, F. C., Perez, M., Singhal, A. K., Hakomori, S., and Paulson, J. C. (1990) *Science* **250,** 1130–1132
7. Walz, G., Aruffo, A., Kolanus, W., Bevilacqua, M., and Seed, B. (1990) *Science* **250,** 1132–1135
8. McEver, R. P., Moore, K. L., and Cummings, R. D. (1995) *J. Biol. Chem.* **270,** 11025–11028
9. Fox, N., Damjanov, I., Martinez-Hernandez, A., Knowles, B., and Solter, D. (1981) *Dev. Biol.* **83,** 391–398
10. Pennington, J. E., Rastan, S., Roelcke, D., and Feizi, T. (1985) *J. Embryol. Exp. Morphol.* **90,** 335–361
11. Fenderson, B. A., Holmes, E. H., Fukushi, Y., and Hakomori, S.-I. (1986) *Dev. Biol.* **114,** 12–21
12. Szulman, A. E., and Marcus, D. M. (1973) *Lab. Invest.* **28,** 565–574
13. Solter, D., and Knowles, B. B. (1978) *Proc. Natl. Acad. Sci. U. S. A.* **75,** 5565–5569
14. Gooi, H. C., Feizi, T., Kapadia, A., Knowles, B. B., Solter, D., and Evans, M. J. (1981) *Nature* **292,** 156–158
15. Eggens, I., Fenderson, B., Toyokuni, T., Dean, B., Stroud, M., and Hakomori, S. (1989) *J. Biol. Chem.* **264,** 9476–9484
16. Lowe, J. B. (1991) *Semin. Cell Biol.* **2,** 289–307
17. Weinstein, J., Lee, E. U., McEntee, K., Lai, P., and Paulson, J. C. (1987) *J. Biol. Chem.* **262,** 17735–17743
18. Cummings, R. D., and Mattox, S. A. (1988) *J. Biol. Chem.* **263,** 511–519
19. Kumar, R., Potvin, B., Muller, W. A., and Stanley, P. (1991) *J. Biol. Chem.* **266,** 21777–21783
20. Lowe, J. B., Kukowska-Latallo, J. F., Nair, R. P., Larsen, R. D., Marks, R. M., Macher, B. A., Kelly, R. J., and Ernst, L. K. (1991) *J. Biol. Chem.* **266,** 17467–17477
21. Goelz, S. E., Hession, C., Goff, D., Griffiths, B., Tizard, R., Newman, B., Chi-Rosso, G., and Lobb, R. (1990) *Cell* **63,** 1349–1356
22. Atchison, M. L., and Perry, R. P. (1987) *Cell* **48,** 121–128
23. Old, L., Boyse, E., and Stockert, E. (1965) *Cancer Res.* **25,** 813–819
24. Hamano, T., and Asofsky, R. (1983) *J. Immunol.* **130,** 2027–2032
25. Hummel, M., Berry, J. K., and Dunnick, W. (1987) *J. Immunol.* **138,** 3539–3548
26. Singer, D., Cooper, M., and Maniatis, T. M. (1974) *Proc. Natl. Acad. Sci. U. S. A.* **71,** 2668–2670
27. Weber, B. L., Westin, E. H., and Clarke, M. F. (1991) *Science* **249,** 1291–1293
28. Raschke, W. C., Baird, S., Ralph, P., and Nakoinz, I. (1978) *Cell* **15,** 261–267
29. Ralph, P., and Nakoinz, I. (1977) *J. Immunol.* **119,** 950–954
30. Koren, H. S., Handwerger, B. S., and Wunderlich, J. R. (1975) *J. Immunol.* **114,** 894–897
31. Fukushima, K., Hirota, M., Terasaki, P. I., Wakisaka, A., Togashi, H., Chia, D., Suyama, N., Fukushi, Y., Nudelman, E., and Hakomori, S. I. (1984) *Cancer Res.* **44,** 5279–5285
32. Galton, J., Terasaki, P. I., Wakisaka, A., Chia, D., Katz, D., and Hardiwidjaja, S. (1985) *A Monoclonal Antibody Reactive with Colonic, Gastric, and Pancreatic Adenocarcinomas, Ninth Int. Convoc. Immuno., Amherst, New York,* pp. 117–125, Karger, Basel, Switzerland
33. Chia, D., Terasaki, P. I., Suyama, N., Galton, J., Hirota, M., and Katz, D. (1985) *Cancer Res.* **45,** 435–437
34. Ernst, L. K., Rajan, V. P., Larsen, R. D., Ruff, M. M., and Lowe, J. B. (1989) *J. Biol. Chem.* **264,** 3436–3447
35. Feinberg, A. P., and Vogelstein, B. (1983) *Anal. Biochem.* **132,** 6–13
36. Kukowska-Latallo, J. F., Larsen, R. D., Rajan, V. P., and Lowe, J. B. (1990) *Genes & Dev.* **4,** 1288–1303
37. Maniatis, T., Fritsch, E. F., and Sambrook, J. (1982) *Molecular Cloning: A Laboratory Manual*, Cold Spring Harbor Laboratory, Cold Spring Harbor, NY
38. Devereux, J., Haeberli, P., and Smithies, O. (1984) *Nucleic Acids Res.* **12,** 387–395
39. Larsen, R. D., Rajan, V. P., Ruff, M. M., Kukowska-Latallo, J., Cummings, R. D., and Lowe, J. B. (1989) *Proc. Natl. Acad. Sci. U. S. A.* **86,** 8227–8231
40. Valanila, R. P., Larsen, R. D., Ajmera, S., Ernst, L. K., and Lowe, J. B. (1989) *J. Biol. Chem.* **19,** 11158–11167
41. Committee on Biological Chemistry, Division of Chemistry and Chemical Technology (1972) *Specifications and Criteria for Biochemical Compounds*, 3rd Ed., National Academy of Sciences, National Research Council, Washington, D. C.
42. Paulson, J. C., Rearick, J. I., and Hill, R. L. (1977) *J. Biol. Chem.* **252,** 2363–2371
43. Mellis, S. J., and Baenziger, J. U. (1983) *Anal. Biochem.* **134,** 442–449
44. Weston, B. W., Smith, P. L., Kelly, R. J., and Lowe, J. B. (1992) *J. Biol. Chem.* **267,** 24575–24584
45. Copeland, N. G., and Jenkins, N. A. (1991) *Trends Genet.* **7,** 113–118
46. Jenkins, N. A., Copeland, N. G., Taylor, B. A., and Lee, B. K. (1982) *J. Virol.* **43,** 26–36
47. Shapiro, S. D., Griffin, G. L., Gilbert, D. J., Jenkins, N. A., Copeland, N. G., Welgus, H. G., Senior, R. M., and Ley, T. J. (1992) *J. Biol. Chem.* **267,** 4664–4671
48. Green, E. L. (1981) *Genetics and Probability in Animal Breeding Experiments*, pp. 77–113, Oxford University Press, New York
49. Dayhoff, M. O. (1978) *Atlas of Protein Sequence and Structure*, Vol. 5, Suppl. 3, National Biomedical Research Foundation, Washington, D. C.
50. Gribskov, M., and Burgess, R. R. (1986) *Nucleic Acids Res.* **14,** 6745–6763
51. Kozak, M. (1989) *J. Cell Biol.* **108,** 229–241
52. Kyte, J., and Doolittle, R. F. (1982) *J. Mol. Biol.* **157,** 105–132
53. Paulson, J. C., and Colley, K. J. (1989) *J. Biol. Chem.* **264,** 17615–17618
54. Natsuka, S., Gersten, K. M., Zenita, K., Kannagi, R., and Lowe, J. B. (1994) *J. Biol. Chem.* **269,** 16789–16794
55. Sasaki, K., Kurata, K., Funayama, K., Nagata, M., Watanabe, E., Ohta, S., Hanai, N., and Nishi, T., (1994) *J. Biol. Chem.* **269,** 14730–14737
56. Weston, B. W., Nair, R. P., Larsen, R. D., and Lowe, J. B. (1992) *J. Biol. Chem.* **267,** 4152–4160
57. Mollicone, R., Candelier, J., Mennesson, B., Couillin, P., Venot, A. P., and Oriol, R. (1992) *Carbohydr. Res.* **228,** 265–276
58. Mollicone, R., Gibaud, A., Francois, A., Ratcliffe, M., and Oriol, R. (1990) *Eur. J. Biochem.* **191,** 169–176
59. Joziasse, D. H., Shaper, N. L., Kim, D., Van den Eijnden, D. H., and Shaper, J. H. (1992) *J. Biol. Chem.* **267,** 5534–5541
60. Joziasse, D. H., Schiphorst, W. E., Koeleman, C. A., and Van den Eijnden, D. H. (1993) *Biochem. Biophys. Res. Commun.* **194,** 358–367
61. Joziasse, D. H., Shaper, J. H., Jabs, E. W., and Shaper, N. L. (1991) *J. Biol. Chem.* **266,** 6991–6998
62. Geurts Van Kessel, A., Tetteroo, P., Van Agthoven, T., Paulussen, R., Van Dongen, J., Hagemeijer, A., and Von Dem Borne, A. (1984) *J. Immunol.* **113,** 1265–1269
63. Reguigne, I., James, M. R., Richard, C. W., III, Mollicone, R., Seawright, A., Lowe, J. B., Oriol, R., and Couillin, P. (1994) *Cytogenet. Cell Genet.* **66,** 104–106
64. Berg, E. L., Robinson, M. K., Mansson, O., Butcher, E. C., and Magnani, J. L. (1991) *J. Biol. Chem.* **266,** 14869–14872
65. Takada, A., Ohmori, K., Takahashi, N., Tsuyuoka, K., Yago, A., Zenita, K., Hasegawa, A., and Kannagi, R. (1991) *Biochem. Biophys. Res. Commun.* **179,** 713–719
66. Saitoh, O., Wang, W.-C., Lotan, R., and Fukuda, M. (1992) *J. Biol. Chem.* **267,** 5700–5711
67. Shaper, N. L., Hollis, G. F., Douglas, J. G., Kirsch, I. R., and Shaper, J. H. (1988) *J. Biol. Chem.* **263,** 10420–10428
68. Nakazawa, K., Ando, T., Kimura, T., and Narimatsu, H. (1988) *J. Biochem. (Tokyo)* **104,** 165–168
69. Lance, P., Lau, K. M., and Lau, J. T. Y. (1989) *Biochem. Biophys Res. Commun.* **164,** 225–232
70. Fitch, W. M., and Margoliash, E. (1970) *Evol. Biol.* **4,** 67–109
71. Sueyoshi, S., Tsuboi, S., Sawada-Hirai, R., Dang, U. N., Lowe, J. B., and Fukuda, M. (1994) *J. Biol. Chem.* **269,** 32342–32350
72. Goelz, S., Kumar, R., Potvin, B., Sundaram, S., Brickelmaier, M., and Stanley, P. (1994) *J. Biol. Chem.* **269,** 1033–1040
73. Smith, D. F., Larsen, R. D., Mattox, S., Lowe, J. B., and Cummings, R. D. (1990) *J. Biol. Chem.* **265,** 6225–6234
74. Ito, K., Handa, K., and Hakomori, S. (1994) *Glycoconj. J.* **11,** 232–237
75. Paulson, J. C., Weinstein, J., and Schauer, A. (1989) *J. Biol. Chem.* **264,** 10931–10934
76. O'Hanlon, T. P., Lau, K. M., Wang, X., and Lau, J. T. Y. (1989) *J. Biol. Chem.* **264,** 17389–17394
77. Shaper, N. L., Wright, W. W., Shaper, J. H. (1990) *Proc. Natl. Acad. Sci. U. S. A.* **87,** 791–795
78. Shaper, N. L., Hollis, G. F., Douglas, J. G., Kirsch, I. R., and Shaper, J. L. (1988)
J. Biol. Chem. **263,** 10420–10428
79. Kitagawa, H., and Paulson, J. C. (1994) *J. Biol. Chem.* **269,** 17872–17878